QFT FOR THE DESIGN OF ACTIVE MAGNETIC BEARING CONTROL SYSTEMS

Z. Y. Wu, C. M. Bingham, D. Howe and D. Peel
Department of Electrical & Electronic Engineering, University of Sheffield, UK.

ABSTRACT
The paper describes the application of Quantitative Feedback Theory (QFT) to the control of active magnetic bearing systems (AMB's). In order to provide a practical focus to the study, the magnetic bearing system of a high-speed energy storage flywheel is considered. QFT templates are employed to specify multi-objective performance constraints for the closed-loop AMB systems to accommodate stability robustness, static and dynamic stiffness requirements, closed-loop bandwidth criterion, the finite power capabilities of the electronic amplifiers, and disturbance rejection properties. Subsequently, the design of various compensation schemes, based on loop-shaping, which satisfy the QFT performance boundaries, and hence, impose the desired attributes on the closed-loop system, is described. Experimental realisation of the resulting compensators to control the AMB's which support the flywheel rim validate the theoretically predicted attributes of the closed-loop system. Thus, QFT is shown to be a very effective methodology for the design of controllers for active magnetic bearing systems.

INTRODUCTION
Due to their contact-less operation, Active Magnetic Bearings (AMB's) are being employed increasingly, particularly in high speed applications and in environments which are subject to wide temperature and pressure variations. The ability to provide vibration control and unbalance compensation also lends AMB's to high precision control applications, and to systems operating in dynamic environments, such as electric vehicles.

The most common force control mechanism for AMB systems is by controlling current in the electromagnets, which also reduces modelling complexity by reducing the effects of winding inductance and resistance variations (via the power amplifier). Whilst this is considered to be an indirect method of control, it can be shown that, for most applications, flux (magnitude) attenuation and phase-delay, stemming from eddy current effects, are negligible over the dynamic bandwidth of the bearing. Thus, in practice, current control can often be as effective as flux control, provided the power amplifiers are properly specified.

This paper focuses on the design of a position controller for an AMB which is employed to support the rim of a flywheel energy storage system, with control of the current in the electromagnets adopted for force control. In order to obtain a linear current vs. force characteristic, differential bias currents are employed on opposing electromagnets, thereby enabling electromagnetic force to be modelled as being proportional to the coil current about the nominal rotor position, and facilitating the use of linear controller design methodologies for position control of the rim. An alternative strategy is to model the non-linear current vs. force vs. position characteristics of the AMB, and resort to non-linear control system design techniques. For example, Feedback Linearization [7], in which a non-linear inner-loop 'linearizing' controller is employed to provide linear system characteristics for the subsequent design of an outer-loop compensator to provide design performance attributes. More commonly, however, linear control system design methods are employed under the assumption that the suspended body does not appreciably deviate beyond the nominal operating region [1, 2, 3, 4, 5, 6].

This paper considers the attributes of Quantitative Feedback Theory (QFT) for the control of AMB's. Compared to other design methodologies, QFT readily incorporates parametric uncertainty, disturbance rejection, stability robustness, and closed-loop performance criteria in a straightforward, graphical manner, whilst offering the designer flexibility in the choice a control structure and complexity.

QUANTITATIVE FEEDBACK THEORY (QFT)
As a continuation of the pioneering work of Bode, Nyquist, Nichols, and others, Horowitz [8] introduced a frequency domain design methodology which was refined in the 1970's to its present form, commonly referred to as Quantitative Feedback Theory (QFT). QFT is based on the use of feedback to provide closed-loop stability robustness in the event of parameter uncertainty and disturbances in the open-loop system, with the addition of an input filter to shape the closed-loop time-domain/frequency-domain performance dynamics. Adoption of QFT by designers has been slow, perhaps due to the graphical nature of the design procedure, however, with dedicated software packages now making graphical manipulation relatively easy, QFT is likely to attract significant attention in the near future.

For a linear plant without dynamic uncertainty, a definite magnitude and phase-shift at any given frequency can be obtained for the open-loop system transfer function. However, when dynamic uncertainty is present, a set of

magnitudes and phase-shifts are obtained at any given frequency; the set being collectively termed a *template*. Using templates, uncertain open-loop system dynamics can be expressed using parametric or non-parametric models, or directly by frequency response measurements, and constitutes one of the key features of QFT-based design.

Here, QFT is used to address the problem of robust stabilisation of AMB's, to support the rim of an energy storage flywheel system, Figure 1. Design details of the flywheel system can be found in previous publications, [9], and will not be expounded here; since the paper concentrates on the controller design issues.

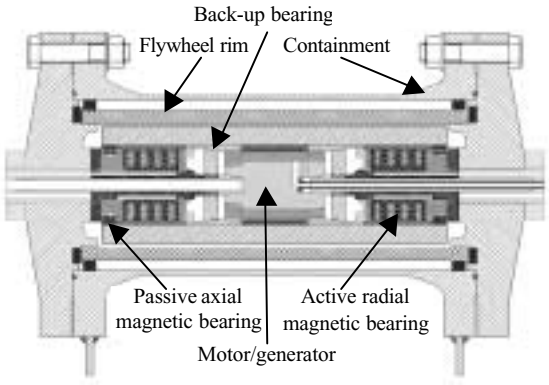

FIGURE 1: AMB's in a flywheel energy storage system.

DYNAMIC MODELLING OF AN AMB

A simplified structure of an AMB position control system is given in Figure 2, in which the rotor is assumed to be a rigid floating body, and the dynamics of the open-loop AMB and controller are denoted by P and G, respectively. The system is subject to force and output disturbances, f_d and x_n, respectively.

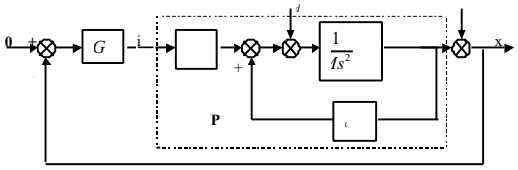

FIGURE 2: AMB control system

A single AMB consists of two opposing electromagnets, one either side of the body to be suspended, supplied by current amplifiers to produce the electromagnetic force. The current in each coil is comprised of a steady-state bias current on which a controller demanded current is superimposed. The transfer function between the control current and the rotor position displacement is:

$$P = \frac{k_i}{Ms^2 + k_x} \qquad (1)$$

where

$$\begin{cases} k_i = 4\mu_0 AN^2 \dfrac{i_0}{x_0^2} \\ k_x = 4\mu_0 AN^2 \dfrac{i_0^2}{x_0^3} \end{cases} \qquad (2)$$

and μ_0 is the permeability of free-space, A is the bearing pole-face area, N is the number of turns on each electromagnet coil, x_0 is the bearing air-gap when the rotor is at its central position, i_0 is the bias current, and M is the effective rotor mass at the AMB. The parameters for the flywheel AMB studied in this paper are given in Table 1.

TABLE 1. System parameters for the flywheel AMBs.

Rotor mass	m	12 kg
AMB pole area	A	$2.6\times10^{-4}\ m^2$
Number of turns/coil	N	40
Nominal air-gap	x_0	0.4 mm
Bias current	i_0	5 A
Permeability of free space	μ_0	$4\pi\times10^{-7}$ H/m

Eq.2 constitutes a linearised model of the flywheel AMB. However, if it is assumed that the control current varies within [-0.9,0.9]*i_0, and the bearing air-gap length on one side changes within [0.2mm, 0.6mm] limited by the mechanical back-up bearing, then the associated parameter variations are shown in Figure 3.

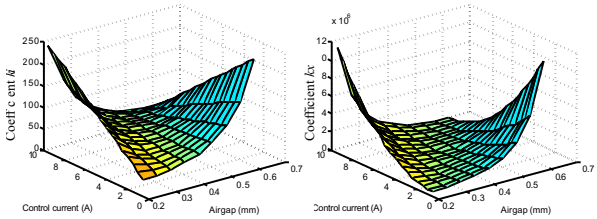

FIGURE 3: Variations of AMB parameters, k_i and k_x.

Thus, the linearised model with bias current, as given by Eq. 1, has a significant uncertainty in terms of the parameters of k_i and k_x. An appropriate controller must, therefore, ensure system stability and satisfy desired closed-loop performance criteria over the range of parameter variations.

The simple linear model of the AMB, Eq.1, is often considered sufficient for the design of position control systems in applications where the rotor and stator flexible modes of vibration are not of particular importance. For a flywheel, however, which has a relatively high rotational speed, the rigid body model does not contain sufficient dynamic detail, and flexible modes of vibration need to be included. The rotor rim has been specifically designed to have the first flexible mode of vibration at a frequency (≈2kHz) significantly higher than the maximum rotational frequency of the rotor rim (1kHz).

Thus, in this case, only the rigid body mode of the rotor needs to be addressed. However, the relatively long axial length and small diameter of the stator means that the first bending mode of the internal stator must be included; and results in the model shown in Figure 4 for controller design purposes.

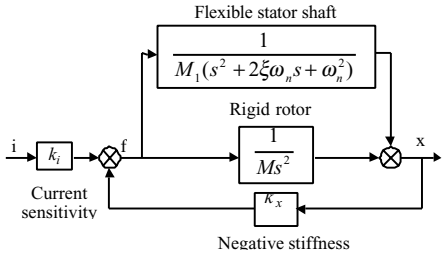

FIGURE 4: AMB dynamic model including the stator first flexible mode of vibration.

The modal coefficients of the stator shaft have been obtained from experiments, and are given in Table 2.

TABLE 2: Modal coefficients of flywheel stator shaft

Mass	M_1=18 kg
Resonance frequency	$\omega_n \approx 1440\ rad/s$
Damping ratio	$\xi = 0.016$

ROBUST CONTROL USING QFT

As with any feedback controller, the primary objective is to impart stability on the closed-loop system, and, theoretically, any linear system can be stabilised using a forward path compensation scheme, regardless of its open-loop stability characteristics. In practice, however, the system is subject to parametric variations, disturbances, and physical limits on the magnitude and bandwidth of the possible control action, and consequently, other performance related specifications must be addressed when a control system is specified. For AMB systems, the satisfactory attainment of at least four stability and performance criteria are sought from the closed-loop system by an appropriately designed controller:

i) Robust Stability

AMBs are inherently unstable, and the full Nyquist Stability Criteria must be invoked to assess closed-loop stability. The AMB must maintain its stability properties subject to the full range of parameteric variations and unmodelled dynamics. To accommodate these desirable characteristics, a constraint on the peak magnitude of the complementary sensitivity function, $T(j\omega)$, for the range of potential open-loop transfer functions, $P(j\omega)$, described by the QFT templates, can be used. For this example, the peak magnitude of $T(j\omega)$ is chosen as $M_T = 1.2 = 1.58dB$. That is:

$$\left|\frac{PG}{1+PG}\right| < 1.2\ , \quad for\ \omega > 0,\ \forall P \in \text{ template} \quad (3)$$

ii) Control Effort Constraints

As regards the finite electromagnetic force capability of the AMBs and the maximum output current capability and bandwidth of the power amplifiers, consideration must be given to limiting the required control effort. Here, the chosen methodology is to limit the effective gain of the controller such that as the flywheel rim traverses its position boundaries over a band-limited range of frequencies, the derived control signal does not exceed its saturation level. For example, for a 0.2mm displacement amplitude at frequencies up to 400rad/s the peak control current is required to be limited to 10Amps (the maximum amplifier output). That is,

$$\left|\frac{G}{1+PG}\right| < 50\ , \quad for\ \omega < 400\ \text{rad/s} \quad (4)$$

iii) Input Disturbance Rejection

A primary specification of AMB's is the static and dynamic load/force capability, referred to as bearing stiffness. The static stiffness of the bearing is generally limited by the maximum dc force capability of the electromagnets, and can be maximised by incorporating integral action into the controller in order to reduce steady-state errors. Dynamic stiffness is defined as a function of frequency, and specified as the magnitude of the position displacement of the rotating body per unit of applied force. For example, the provision of a dynamic stiffness of $1\times10^8\ N/m$ up to 100 rad/s; i.e., 100N sinusoidal disturbances at frequencies up to 100rad/sec which will result in less than 1µm deflection of the flywheel rim, is described by:

$$\left|\frac{X}{f_d}\right| < 1\times10^{-8}\ , \quad for\ \omega < 100\ rad/s \quad (5)$$

which, for QFT controller design purposes, can be translated to the more amenable form:

$$\left|\frac{P}{1+PG}\right| < 0.001\ , \quad for\ \omega < 100\ rad/s \quad (6)$$

iv) Output Disturbance Attenuation

The controller can also be designed to accommodate output disturbances (which are normally of a relatively low frequency nature), impose desired static stiffness properties to the AMB, and be designed to provide a desired closed-loop bandwidth, by bounding the sensitivity function, $S(j\omega)$. An example specification is:

$$\left|\frac{X}{X_n}\right| = \left|\frac{1}{1+PG}\right| = |S| < |0.009\omega|\ , \quad for\ \omega < 100\ rad/s \quad (7)$$

which requires $S(j\omega)$ to have infinite attenuation at low frequencies, or, conversely, $G(j\omega)$, to provide infinite magnitude. This, in turn, necessitates the inclusion of integral action in the controller, and, hence, provides high bearing stiffness under constant force disturbances. An estimate of the closed-loop bandwidth, ω_b, is the frequency at which $|S|$ first crosses $1/\sqrt{2}$ (=-3dB) from below, and, in this case, a lower bound on the bandwidth

is ≈80rad/s. The trade-off between a high ω_b, which also provides low frequency output disturbance rejection, and the finite limits of control action, often constitute the dominant performance compromise for the design of the loop-shape $L(j\omega)=G(j\omega)P(j\omega)$.

All these desired performance specifications can be translated onto magnitude vs. phase plots (Nichols charts), as a function of frequency. However, by enabling the multiple design constraints, the performance can be reduced to a single set of 'worst-case' performance boundaries, Figure 5. The objective of QFT design is to loop-shape $P(j\omega)G(j\omega)$, by appropriate choice of $G(j\omega)$, such that at each frequency a template has been generated and a performance boundary obtained, such that the magnitude and phase-shift of the nominal loop transfer function lies 'above' the respective performance boundary. Clearly, this can be tedious when attempting to satisfy all the performance objectives. However, the task can be eased by employing graphical software packages (eg. Matlab/Simulink QFT toolbox).

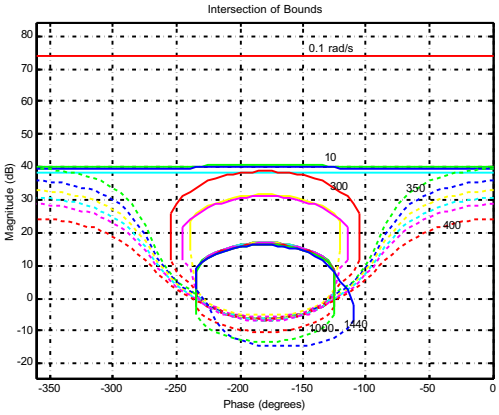

FIGURE 5: Intersection of performance boundaries

COMPENSATOR DESIGN USING QFT

The flywheel rim is supported by 4 radial, homopolar, active magnetic bearings with a peak force capability of 1600N on the vertical axis and 800N on the horizontal axis. Eddy current displacement sensors are used for position control of the active bearing on each radial axis, the sensors having a resolution of $1\mu m$, a linearity of 1% of full scale, and a bandwidth of 5kHz. To facilitate rapid control system development, a DSPACE/TMS320C40-based hardware development platform is employed to realise the designed compensators. Three compensators have been designed with varying degrees of complexity, viz. design for robust stability, design for robust stability and high static stiffness, and a high-order compensator to accommodate all the performance objectives previously described.

Compensator Design For Robust Stability

The simplest form of compensator for AMB's is based on the incorporation of derivative action to provide the required degree of damping to the closed-loop dynamics, with the addition of proportional action to the control bearing stiffness. In practice, due to high frequency noise from the switched-mode power amplifiers, and measurement noise, a low-pass filter is incorporated after the derivative element so as to reduce unwanted amplification of out-of-band frequencies; thereby resulting in a phase-lead compensation scheme.

Consider the requirement for robust stability:

$$\left|\frac{PG}{1+PG}\right| < 1.2\,, \quad for\ \omega > 0 \tag{8}$$

Figure 6(a) shows the result of an iterative loop-shaping design procedure to satisfy the robust stability performance boundaries at each frequency, the compensator, $G(s)$, being given by:

$$G(s) = \frac{4000\,(s+360)}{(s+5000)} \tag{9}$$

It is noted that the structure of this compensator has also been the result of other design methodologies, for example, involving robust eigenstructure assignment [1].

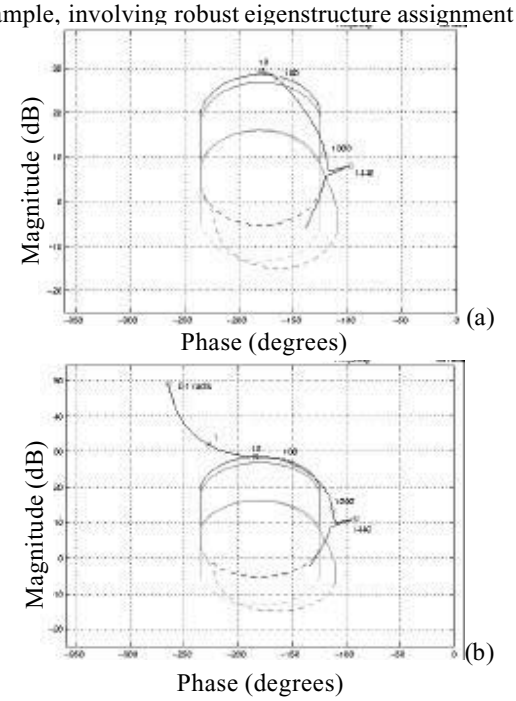

FIGURE 6: QFT loop-shape design to satisfy robust stability criterion (a) PD-type compensation, (b) PID-type compensation.

Whilst manufacturing tolerances mean the dynamics of each AMB differs from that of the other AMB's, and the system of four AMBs form an inherently multivariable control problem, this study is focused on the application of $G(s)$ to each of the four axes to support the rim. Step responses of the simultaneous initial excitation of all four AMB's are given in Figure 7, and show transient overshoots of up to 33%. This 'worst-case' result is a consequence of dynamic multivariable cross-coupling, which is not accounted for in the design procedure, and which accentuates overshoot due to the dominant acceleration of one side of the flywheel rim. However,

on average the overshoot is ≈10%, which is commensurate with the requirement $M_T<1.2$. It is also noted that steady-state errors are present on all axes.

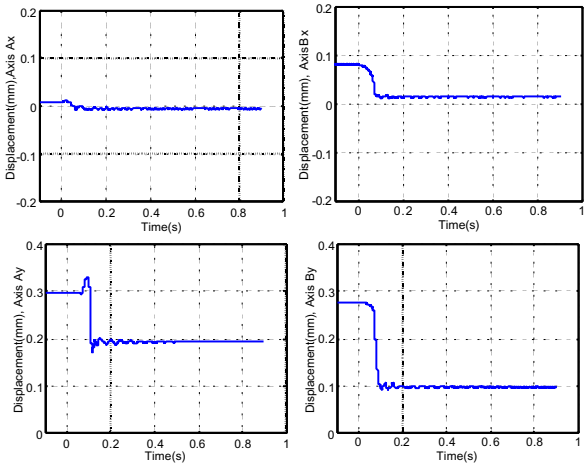

FIGURE 7: Measured transient response of flywheel rim with PD-type compensator designed for robust stability.

Design For Robust Stability And Static Stiffness

In order to improve the static stiffness of the AMB, the previous PD-type control structure can be augmented with integral action. Figure 6(b) shows the result of the loop-shaping design process, again to satisfy the robust stability criterion, when the compensator has been designed to incorporate a pure integrator; the resulting compensator given by:

$$G(s) = \frac{1412501976\ (s+230)(s+1.1)}{s(s+2.019\times10^5)(s+6000)} \qquad (10)$$

As in the previous case, additional factors have been added to the compensator to reduce the effects of high frequency noise and to counter the destabilising phase-shift of the integrator (an extra zero at s=-1.1). Implementing *G(s),* and simultaneous excitating all four AMB axes, results in the transient responses shown in Figure 8.

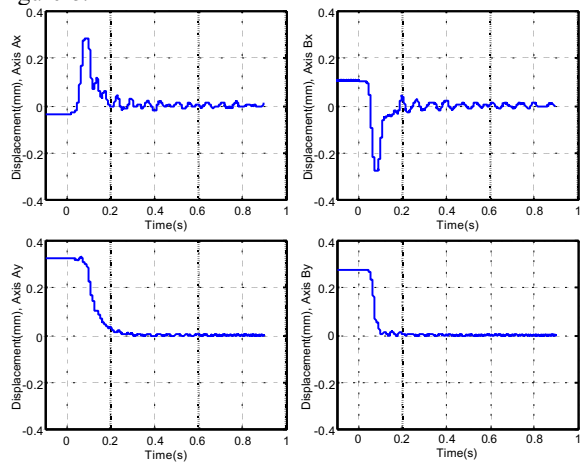

FIGURE 8: Measured transient response of flywheel rim with PID-type compensator designed for robust stability.

It is evident that the integral action has facilitated zero steady-state position error on all axes, a feature which is independent of any constant force applied to the rim (to within the physical limits of the system), and verifies the attainment of a high static-stiffness.

Satisfying All Performance Objectives

As discussed previously, the attainment of other criteria is also important in order to impart desirable closed-loop performance characteristics under the influence of disturbances and limited control action. In this case, loop-shaping is employed to design an appropriate controller to satisfy the combined boundary constraints given in Figure 5. The result of the loop-shaping procedure is shown in Figure 9, where all the performance boundaries have been satisfied by the compensator:

$$G(s) = \frac{5188553(s+1604)(s+5.593)(s^2+477.7s+1.501\times10^5)(s^2+90.94s+1.21\times10^5)}{s(s+400)^2(s+1.182\times10^4)(s+6973)(s+1096)} \qquad (11)$$

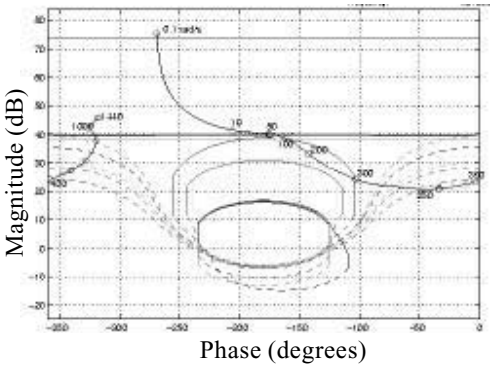

FIGURE 9: QFT loop-shape design to satisfy robust performance boundaries.

Implementing *G(s)* and simultaneously excitating all the AMB's, results in the transient responses shown in Figure 10. They show that zero steady-state position error and the desired closed-loop bandwidth characteristics have been obtained with limited control action, as desired.

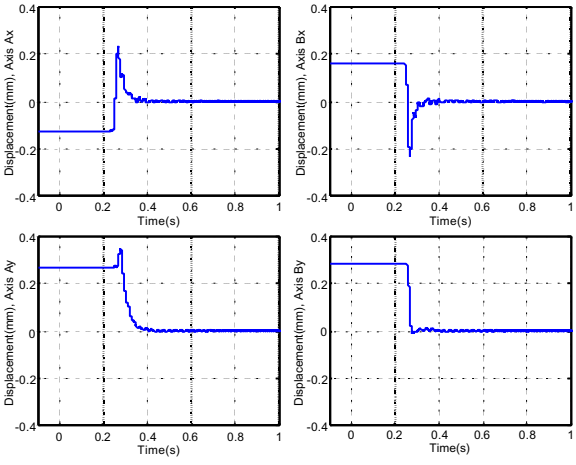

FIGURE 10: Measured step responses of flywheel AMB's with high-order compensator.

In order to assess the dynamic stiffness of the AMB's, the transmission of exogenous disturbance noise, f_d, to the output, x, is tested by striking the suspended flywheel rim with a modal impulse hammer and analysing the frequency response using a spectrum analyser. The resulting frequency response transfer characteristic, Figure 11, shows that disturbances are attenuated by at least -60dB up to 100rad/sec, and verifies that the input disturbance rejection specification has been met.

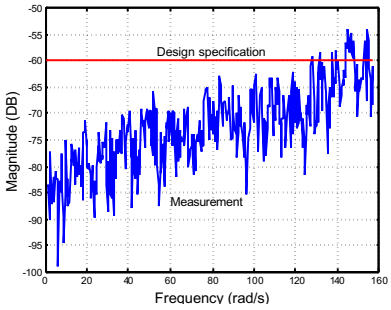

FIGURE 11: Measured frequency response $\frac{x(j\omega)}{f_d(j\omega)}$.

The QFT design method has also been applied to a flywheel energy storage system with a sightly modified stator. Figure 11 presents the performance of the magnetic bearings when the flywheel rim was rotating at speeds up to 10,000rpm. It will be observed that the system passes safely through the first critical speed (resonant frequency) in a controlled manner, during both the run-up and run-down of the flywheel.

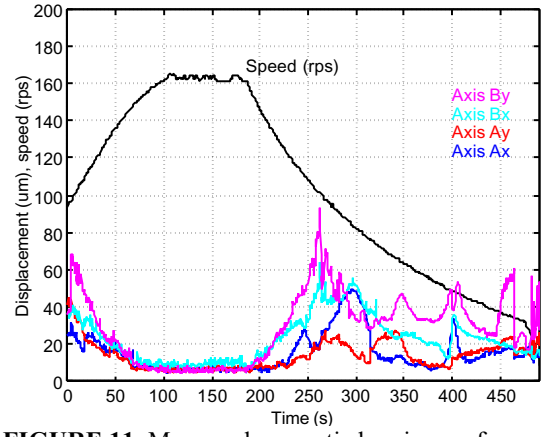

FIGURE 11: Measured magnetic bearing performance with the flywheel rotating at speeds up to 10,000rpm.

CONCLUSIONS

The paper has considered the application of Quantitative Feedback Theory (QFT) to the control of active magnetic bearing systems. There application to support the high-speed rim of a flywheel energy storage system has provided a platform for experimental verification of the theoretical design studies. It has been shown that QFT can readily be employed to accommodate the primary characteristics (robust stability, input/output disturbance attenuation, control effort constraints) sought from closed-loop control of AMB's, by use of *templates* to produce a combined set of frequency domain performance boundaries. Loop-shaping has subsequently been employed to modify the loop transfer function in order to satisfy the boundary constraints.

Comprehensive design studies have been presented to show the progressive development of compensators to promote robust stability and other performance objectives, viz. static and dynamic bearing stiffness, input/output disturbance rejection, and restrictions on amplifier current and bandwidth; the performance of the controllers being verified by experiment.

Research is currently underway to accommodate the multivariable interaction between the AMB's of the flywheel, and to include higher order flexible modes, using QFT design methodologies. The results of this work will be published in due course.

ACKNOWLEDGEMENTS

The authors gratefully acknowledge the provision of funding from the European Commission, under the BRITE-EURAM and JOULE-THERMIE programmes, to support research on energy storage flywheel systems for use in electric vehicles, of which the work reported in the paper forms a small part.

REFERENCES

1. Duan, G.R., Wu, Z.Y., Bingham, C.M., Howe, D.:'Robust magnetic bearing control using stabilizing dynamic compensators'; Proc. IEMDC'99, Seattle, USA, pp. 493-495.
2. Matsumura F., Namerikawa T., Hagiwara K. and Fujita M.: 'Application of gain scheduled H_∞ robust controllers to a magnetic bearing'; IEEE Transactions on Control Systems Technology, 4(5), 1996, pp. 484-493.
3. Nonami K and Ito T.: 'μ-synthesis of flexible rotor magnetic bearing systems'; IEEE Transactions on Control Systems Technology, 4(5), 1996, pp. 503-512.
4. Schroder P, Green B. and Fleming P. J.: 'On-line genetic auto-tuning of magnetic bearing controllers'; proc. ISMB-6, Boston, Aug. 1998, pp.321-330.
5. Schweitzer G., Bleuler H. and Traxler A.: 'Active magnetic bearings, basic, properties and applications'; Zurich, Switzerland, vdf Hochschulverlag AG, 1994.
6. Shafai B., Beale S., LaRocca P. and Cusson E.: 'Magnetic bearing control systems and adaptive forced balancing'; IEEE Control Systems, April 1994, pp. 4-13.
7. Trumper D. L., Olson S. M. and Subrahmanyan P. K.:'Linearizing control of magnetic suspension systems'; IEEE Transactions on Control System Technology, 5(4), 1997, pp. 427-438.
8. Horowitz I. M.: 'Synthesis of feedback systems', Academic Press, New York, 1963.
9. Howe D., Mason P. E., Mellor P. H., Wu Z. Y. and Atallah K.: 'Flywheel peak power buffer for electric/hybrid vehicles'; IEEE International Electric Machines and Drives Conference , IEMDC'99, Seattle, Washington, USA, May 9-12, 1999, pp. 508-510.